Autophosphorylation of Threonine 485 in the Activation Loop Is Essential for Attaining eIF2α Kinase Activity of HRI†

Maryam Rafie-Kolpin,‡ An-Ping Han, and Jane-Jane Chen*

Harvard−MIT Division of Health Sciences and Technology, Massachusetts Institute of Technology, 77 Massachusetts Avenue, Cambridge, Massachusetts 02139

Received January 3, 2003; Revised Manuscript Received March 27, 2003

ABSTRACT: In heme deficiency, protein synthesis is inhibited by the activation of the heme-regulated eIF2α kinase (HRI) through its multiple autophosphorylation. Autophosphorylation sites in HRI were identified in order to investigate their functions. We found that there were eight major tryptic phosphopeptides of HRI activated in heme deficiency. In this report we focused on the role of autophosphorylation at Thr483 and Thr485 in the activation loop of HRI. Disruption of the autophosphorylation of Thr485, but not Thr483, resulted in a lower autokinase activity and locked Thr485Ala HRI in a hypophosphorylated state. Most importantly, autophosphorylation of Thr485, but not Thr483, was essential for attaining eIF2α kinase activity of HRI. In addition, autophosphorylation of Thr485 was necessary for arsenite-induced activation of the eIF2α kinase activity of HRI, while autophosphorylation at Thr483 was not required for activation by arsenite. The function of Thr490, another conserved Thr residue in the activation loop of HRI, was also investigated. Mutations of Thr490 to either Ala or Asp resulted in reduced autokinase activity and loss of eIF2α kinase activity in heme deficiency or upon arsenite treatment. Since Thr490 was not identified as an autophosphorylated site, it is likely that Thr490 itself might be critical for the catalytic activity of HRI. Importantly, Thr485 was very poorly phosphorylated in Thr490 mutant HRI. Collectively, our results demonstrate that autophosphorylation of Thr485 is essential for the hyperphosphorylation and activation of HRI and is required for the acquisition of the eIF2α kinase activity.

In heme deficiency, protein synthesis in reticulocytes is inhibited by the activation of the heme-regulated eIF2α kinase (HRI)[1] and the subsequent phosphorylation of eIF2α. The activation of HRI is accompanied by its autophosphorylation (*1*−*3*). While eIF2 is the initiation factor that binds GTP and Met-tRNA$_f$ and forms the 43S preinitiation complex, the recycling of eIF2 requires the exchange of GDP for GTP. Under physiological conditions, the affinity of eIF2 for GDP is 400-fold higher than for GTP. The exchange reaction is catalyzed by eIF2B, which is rate limiting and present at 15−20% of the amount of eIF2 in reticulocytes. The phosphorylation of eIF2α by its kinases renders eIF2B nonfunctional and shuts off protein synthesis (*3*−*6*).

We have shown recently by targeted disruption of the HRI gene in mice that HRI is essential for the translational regulation and the survival of erythroid precursors in iron deficiency (*7*). The rate of protein synthesis in HRI$^{-/-}$ reticulocytes is markedly increased in a heme-independent manner as compared to the wild-type reticulocytes. In addition, there is an increase in the larger sized polysomes and decreased eIF2α phosphorylation. These findings provide the in vivo evidence for the function of HRI in regulation of translational initiation of erythroid cells. In iron-deficient HRI$^{-/-}$ mice, protein synthesis continues and the heme-free globins aggregate and precipitate as inclusions in the red blood cell and its precursors, resulting in the accelerated apoptosis of erythroid precursors in the bone marrow and spleen. Thus, HRI serves as a feedback inhibitor in the regulation of the synthesis of α- and *β*-globins when intracellular heme concentration declines. This function of HRI ensures the balanced synthesis of globin chains and their prosthetic group, heme, in the formation of stable hemoglobin.

HRI belongs to the family of eIF2α kinases which includes the double-stranded RNA (dsRNA) dependent eIF2α kinase (PKR) (*8*), the GCN2 protein kinase (*9*−*11*), and the ER resident kinase (PERK) (*12*, *13*). These eIF2α kinases share extensive homology in their kinase catalytic domains and phosphorylate eIF2α at the serine 51 residue (*1*). The regulatory domains and mechanisms of each eIF2α kinase, however, are very different. PKR is activated by dsRNA bindings to the two N-terminal dsRNA binding motifs which promote dimerization and facilitate trans-autophosphorylation (*14*, *15*). GCN2 is activated under amino acid starvation conditions through the C-terminal domain, which closely resembles the histidyl-tRNA synthase. This domain senses the accumulation of uncharged tRNA and is essential for the activation of GCN2 (*16*, *17*). PERK is activated by ER stress through its lumenal domain, which is similar to the sensor domain of the ER stress kinase Ire-1 (*12*). HRI is downregulated by heme through the two heme-binding domains in the N-terminus and kinase insertion region (*18*, *19*).

† This study was supported by U.S. Public Health Service Grant DK-53223 to J.-J.C. from the National Institute of Diabetes and Digestive and Kidney Diseases. M.R.-K. was supported in part by NIH Postdoctoral Fellowship DK-09773.

* Corresponding author. Tel: (617) 253-9674. Fax: (617) 253-3459. E-mail: j-jchen@mit.edu.

‡ Present address: Interleukin Genetics, Inc., Waltham, MA 02452.

[1] Abbreviations: HRI, heme-regulated eIF2α kinase; dsRNA, double-stranded RNA; Wt, wild type; PCR, polymerase chain reaction.

10.1021/bi034005v CCC: $25.00
Published on Web 05/08/2003

Activation of these eIF2α kinases is accompanied by their autophosphorylation. PKR are multiply autophosphorylated at three Ser/Thr residues located between the dsRNA binding domains and the first kinase domain (*20*), seven Ser/Thr residues between the two dsRNA binding domains (*21*, *22*), and eight Ser/Thr residues located in the kinase insertion domain (*21*). Mutations of all of these Ser/Thr to Ala had little effect on the eIF2α kinase activity of PKR. In contrast, autophosphorylation of PKR at Thr446 and Thr451 located in the activation loop has been shown to be required for kinase activity both in vivo and in vitro (*21*, *23*). Similarly, GCN2 autophosphorylates at Thr882 and Thr887 in the activation loop, and the mutation of these residues to Ala also impaired its kinase activity (*23*).

Recently, we have shown that the native HRI in reticulocytes and the recombinant HRI expressed in *Escherichia coli* undergo multiple autophosphorylation at Ser, Thr, and Tyr residues. This multiple autophosphorylation in heme deficiency occurs in two stages. The first stage autophosphorylation is required to prevent aggregation of the inactive ProHRI. The second stage autophosphorylation is required for the formation of the stable, dimeric HRI that is heme-regulated (heme-reversible HRI) (*24*). Using mouse reticulocytes and nucleated erythroid progenitor cells from fetal liver, we have demonstrated recently that HRI is activated in response to several cytoplasmic stress conditions such as oxidative stress, heat shock, and osmotic shock, in addition to heme deficiency. Activation of HRI by these stresses is also achieved through its autophosphorylation (*25*). Furthermore, molecular chaperones, hsp90 and hsp70, are required for the activation of HRI both in heme deficiency (*26*, *27*) and upon stress conditions (*25*).

To define the regulatory function of each of the multiple autophosphorylations of HRI, we have begun to identify these autophosphorylation sites. Here, we report that the HRI was autophosphorylated at Thr483 and Thr485 residues located in the activation loop. We demonstrated by site-directed mutagenesis that autophosphorylation at Thr485, but not Thr483, is essential for the activation of the eIF2α kinase activity of HRI both in heme deficiency and in response to oxidative stress induced by arsenite. In addition, we showed that activated wild-type (Wt) HRI and constitutively active T485D (Asp substitution of Thr485) HRI were no longer regulated by heme.

MATERIALS AND METHODS

Materials. E. coli BL21 cell, pET28a and pTriEx-1 vectors, and Gene-Juice transfection reagents were obtained from Novagen. [^{32}P]Orthophosphoric acid (28.3 Ci/μmol) was purchased from New England Technologies Inc. Sodium arsenite was from Sigma. Ni^{2+}-NTA−agarose was from Qiagen. Tissue culture media and serum were obtained from Gibco Life Technologies and HyClone, respectively. The horseradish peroxidase conjugated second antibody was purchased from Promega. The chemiluminescent reagents were from NEN Life Sciences.

Expression and Purification of the ^{32}P-Labeled HRI in E. coli. Mouse HRI was expressed in *E. coli* BL21 cells as described previously (*24*) with a slight modification. Bacterial culture (50 mL) was grown at 37 °C to a cell density of A_{600} = 0.6 and then induced with 100 μM isopropyl thiogalactoside (IPTG) for HRI expression with the simultaneous addition of 4 mCi of [^{32}P]orthophosphoric acid. Following induction, the growth temperature was reduced to 13 °C. Cells were harvested 8 h later by centrifugation and were washed once with PBS. Cells were resuspended and lysed by sonication in a buffer containing 50 mM NaH_2PO_4, pH 8.0, 300 mM NaCl, 10 mM imidazole, protease inhibitors, 1 mM NaF, 0.1 mM $NaVO_4$, 5 mM 2-mercaptoethanol, and 10% glycerol. After sonication, Triton X-100 was added to cell lysates to a final concentration of 1% and was incubated on ice for 15 min. Detergent-treated cell lysates were centrifuged at 16000*g* for 60 min at 4 °C. The 16000*g* supernatant was loaded to a Ni^{2+}-NTA−agarose column (0.5 mL). The column was washed with 20 mM imidazole in the above-described buffer. Bound HRI was eluted with 250 mM imidazole in the same buffer described above. Purified HRI was pooled and dialyzed against PBS plus 2 mM dithiothreitol (DTT) to remove imidiazole and salt.

Separation of the Phosphopeptides by Two-Dimensional Electrophoresis and Thin-Layer Chromatography. Purified HRI was further separated by 7.5% SDS−PAGE and transferred to a nitrocellulose membrane. The membrane was exposed to X-ray film to locate the [^{32}P]HRI. The strip containing HRI was excised out, incubated with 0.5% PVP-40 in 100 mM acetic acid for 30 min at room temperature, and washed five times with distilled H_2O and then twice with 50 mM freshly prepared ammonium bicarbonate, pH 7.7. HRI in the nitrocellulose was digested with 10 μL of 1 mg/mL TPCK trypsin in 150 μL of ammonium bicarbonate for 2 h at 37 °C. An additional 10 μL of TPCK trypsin was then added, and HRI was further digested overnight at 37 °C.

Deionized water (300 μL) was added to the tryptic digest. The sample was vortexed for 1 min and spun for 5 min at 10000 rpm, and the supernatant was transferred to a new microfuge tube. The HRI digest was dried in a speed-vac, and the pellet was incubated in 50 μL of cold performic acid for 1 h at room temperature. Samples were then dried in a speed-vac, and the dry pellets were washed with distilled water several times until no residual salt precipitates remained on the walls of the tubes. The pellets were dissolved in 300 μL of a pH 1.9 buffer consisting of 1.94% formic acid and 7.8% glacial acetic acid and dried. The dry pellets were dissolved in 10 μL of the pH 1.9 buffer, and 7 μL of the samples was loaded onto cellulose thin-layer plates for phosphopeptide analysis.

Tryptic peptides of HRI were separated using the Hunter thin-layer peptide mapping electrophoresis system as described by Van Der Geer and Hunter (*28*). In the first dimension, tryptic peptides in cellulose plates were separated by electrophoresis at 1250 V for 35 min in a pH 1.9 buffer described above. Plates were air-dried and then subjected to the second dimension thin-layer chromatography in a phospho-chromatography buffer consisting of 37.5% 1-butanol, 25% pyridine, and 7.5% glacial acetic acid for 10 h at room temperature. The individual phosphopeptide in the thin-layer plates was extracted as described (*28*). The eluted phosphopeptides were covalently linked to PVDF membrane according to the procedure provided by Millipore in the Sequelon−AA reagent kit and then subjected to covalent amino acid sequencing by the MIT Biopolymer Laboratory.

Preparation and Expression of HRI Mutants. The codons of Thr483 and Thr485 in mouse HRI cDNA were changed individually from ACA to either GCA for alanine (A) or GAC for aspartic acid (D), and the codon for Thr490 was changed from ACT to GCA for alanine or GAC for aspartic acid by site-directed mutagenesis and recombinant polymerase chain reaction (PCR) techniques (*29*, *30*). The recombinant PCR products spanned between nucleotides 1138−1894 and were flanked by unique *Kpn*I and *Eco*RI sites. After restriction digests with *Eco*RI and *Kpn*I, the cDNA fragments containing the mutations were subcloned into the pET28a bacterial expression vector. The correct mutations were confirmed by DNA sequencing. These HRI mutants, Wt HRI, and the previously prepared inactive K196R mutant (*24*) were expressed in *E. coli* BL21 cells as described above either at 13 °C overnight or at 25 °C for 2 h.

For expression in mammalian cells, Wt HRI cDNA was subcloned into the pTriEx-1 vector at the *Nco*I/*Hin*dIII site. A *Nco*I site was introduced at the 5′ end of the initiation codon of the HRI cDNA. A *Hin*dIII site was also engineered right before the stop codon in mouse HRI cDNA to allow expression of HRI with a C-terminal tag. The PCR product was sequenced to verify that no mistake was introduced during PCR amplification. The C-terminal tag unfortunately reduced the expression and activity of HRI when expressed in either *E. coli* or mammalian cells. To overcome this problem, a stop codon was introduced before the tag by replacing the *Kpn*I/*Hin*dIII HRI cDNA fragment in the pTriEX-1 vector with that from the HRI cDNA in the pET28a vector. To prepare the Thr mutants in pTriEX-1 vectors, the mutated HRI cDNAs in pET28a plasmids were subcloned through *Kpn*I and *Hin*dIII sites. To prepare the inactive K196R mutant, a *Nco*I site was introduced at the 5′ end of the initiation codon of K196R HRI. The region between *Nco*I and *Kpn*I of HRI cDNA was PCR amplified and digested with *Nco*I and *Kpn*I. Wt HRI in pTriEx-1 was digested with *Kpn*I and *Nco*I enzyme and was replaced with the K196R PCR fragment.

The day before transfection, human embryonic kidney 293T cells were plated at 2×10^5 cells in six-well plates. Cells were incubated at 37 °C overnight. Wt, T483, T485, T490, and the inactive K196R mutant HRI plasmids (3−5 μg) were transfected into 293T cells using Gene-Juice transfection reagents and the recommended procedure of the manufacturer. Expressions of HRI proteins were analyzed 24−48 h after transfection. For arsenite stress, cells were trypsinized 24 h after transfection and replated into six-well plates at 2×10^5 cells per well. Cells were allowed to attach to the plates for 24 h and were then treated with or without sodium arsenite (200 μM) for 60 min as described previously (*25*).

*Lysate Preparation, Western Blot Analysis, and eIF2*α *Kinase Assays.* Transfected 293T cells were lysed in 300−500 μL of lysis buffer containing 20 mM Tris-HCl (pH 7.4), 50 mM KCl, 2 mM DTT, 1 mM Na_2EDTA, 1 mM Na_3VO_4, 1 mM NaF, 1 mM β-glycerophosphate, 1× protease inhibitor, 1% NP-40, and 10% glycerol for 15 min at 4 °C. Cell debris was removed by centrifugation at 10000*g* for 5 min at 4 °C. For determination of the status of HRI phosphorylation, cell lysates from an equal number of cells were separated by 7.5% SDS−PAGE and subjected to Western blot analysis of HRI using anti-HRI antibody as described previously (*25*). Western blot analysis of HRI expressed in *E. coli* using anti-P-Ser, anti-P-Thr, and anti-P-Tyr antibodies was performed as described previously by Bauer et al. (*24*). eIF2α kinase assays were performed using the same amount of HRI protein and recombinant yeast eIF2α as the substrate as described previously (*24*).

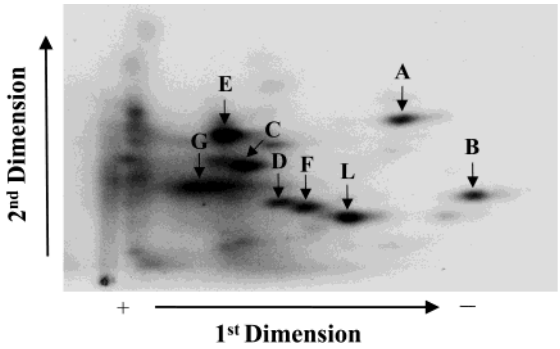

FIGURE 1: Separation of the tryptic phosphopeptides of in vivo labeled HRI. Mouse HRI was labeled in vivo with [^{32}P]orthophosphate during expression in *E. coli* as described in Materials and Methods. Tryptic peptides of HRI were prepared and separated by two-dimensional thin-layer electrophoresis and chromatography. ^{32}P-labeled peptides were visualized by autoradiography. The major ^{32}P-labeled peptides are marked with arrows and letters.

RESULTS

Autophosphorylation of Threonines 483 and 485 of Mouse HRI in Vivo. We have previously shown that recombinant HRI expressed in *E. coli* undergoes multiple autophosphorylation as in native reticulocytes (*24*). Therefore, mouse HRI was expressed in *E. coli* in the absence of exogenous heme and in the presence of [^{32}P]inorganic phosphate to identify the autophosphorylation sites. The major protein phosphorylated under these conditions was HRI that was maximally autophosphorylated. The radioactively labeled HRI was purified by Ni^{2+} column chromatography and processed for exhausted tryptic digestion. The tryptic phosphopeptides of HRI were separated by two-dimensional thin-layer electrophoresis and chromatography. As shown in Figure 1, there were eight major and several minor tryptic phosphopeptides, confirming the multiple autophosphorylation of HRI in heme deficiency (*24*, *31*, *32*).

The major peptides were assigned with letters and were subjected to covalent amino acid sequencing which cleaved one amino acid sequentially from the NH_2 terminus. The cleaved amino acids were collected, and their radioactivities were determined by liquid scintilliation to identify the position of phosphorylated amino acids in the phosphopeptide. The patterns of the positions of phosphorylated amino acids of phosphotryptic peptides were then matched to the amino acid sequence of the predicted tryptic peptides of HRI which contain phosphorylatable Ser, Thr, or Tyr at the positions corresponding to the positions of phosphorylated amino acids. As shown in Figure 2, the covalent amino acid sequencing of phosphopeptide D revealed the presence of phosphorylated residues at the first and the third amino acids. The predicted tryptic peptide of mouse HRI composed of amino acids 483−495 contains a Thr residue at amino acid 483 (position 1) and a Thr residue at amino acid 485 (position 3), matching the position of the phosphorylated amino acid of phosphopeptide D. This is the only match among all HRI tryptic peptides. Thus, these results demonstrate that HRI is autophosphorylated at Thr483 and Thr485 in heme deficiency when expressed in *E. coli*.

Table 1: Conservation of T483 and T485 among HRI from Different Species[a]

	HRI	VII		VIII
			483 485 490	
1	Mouse	-VK**IGDFGLAC**ADIIQNADWTNRNGKGTR-----	**T**H**T**SRV**GTCLYASPEQ**LEGSQYGAKS	
2	Human	-VK**IGDFGLAC**TDILQKNTDWTNRNGKRTP----	**T**H**T**SRV**GTCLYASPEQ**LEGSEYDAKS	
3	Rat	-VK**IGDFGLAC**ADIIQKSADWTNRNGKGTP----	**T**H**T**SRV**GTCLYASPEQ**LEGSEYDAKS	
4	Rabbit	-VK**IGDFGLAC**ADIIQKNAARTSRNGERAP----	**T**H**T**SRV**GTCLYASPEQ**LEGSEYDAKS	
5	Chicken	-VK**IGDFGLAC**KDLLWDDADQWFHTERINGl---	**T**H**T**SGV**GTCLYASPEQ**LQGSDYDFKS	
6	Xenopus	HVR**IGDFGLAC**RDIIQKSRDSWLNKDGSKGA---	**T**H**T**TGV**GTCLYAAPEQ**LKGSRYDFKS	
7	Fish	HVK**IGDFGLAC**XNIIMDEHEKLPSSSQAGVNPDA	**T**H**T**SGV**GTFVYAAPEQ**LEGSRYDSKS	

	446 451	
PKR	KR**T**RSK**GT**LRYM**SPEQ**I	
	882 887	
GCN2	NL**T**SAI**GT**AMYVA**TE**VL	
	980 985	
PERK	TH**T**GQV**GT**KLYM**SPEQ**I	

[a] Sequence alignment of the segment between kinase domains VII and VIII of HRI from seven species is shown here. Invariable residues among all species are marked by bold type. In addition, the conserved T483, T485, and T490 in the activation loop are underlined. The equivalents of T485 and T490 of HRI in other eIF2α kinases, PKR, GCN2, and PERK are also in bold type, underlined, and shown in the bottom.

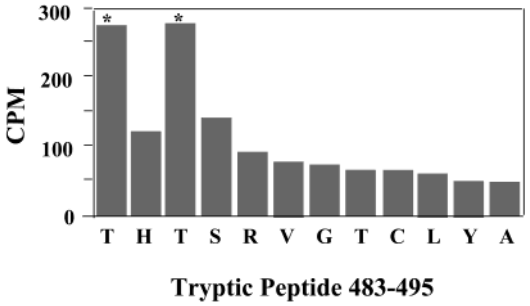

FIGURE 2: T483 and T485 of HRI are autophosphorylated. Phosphopeptide D shown in Figure 1 was subjected to covalent amino acid sequencing. The ^{32}P radioactivity in each fraction was plotted and matched with the amino acid sequence of a tryptic peptide of mouse HRI 483−495.

Phosphopeptides were also enriched by immobilized metal affinity chromatography (*33*, *34*) and subsequently subjected to mass spectrometry. The increase of the molecular mass by the incorporation of phosphates and in the multiples of 80 Da above the mass of tryptic peptides permitted us to identify the number of phosphorylation sites in the potential phosphotryptic peptides. For example, we found a molecular mass of a phosphopeptide of 1075.85 Da, which is 159.9 Da (two phosphates) more than the expected molecular mass of 915.98 Da of the tryptic peptide 482−489 (GTRT^{483}HT^{485}SR). Thus, these methodologies allowed us to further deduce that there were two autophosphorylation sites in this peptide, consistent with the above conclusion of autophosphorylation at T483 and T485.

We have also identified autophosphorylation sites in rabbit HRI expressed in Sf9 cells using the baculovirus expression system. HRI was purified by immunoaffinity chromatography (*18*) and autophosphorylated in vitro. The radioactively labeled HRI was separated by SDS−PAGE and was then excised for in-gel tryptic digest. The tryptic fragments were separated by HPLC, and the ^{32}P radioactivity in each fraction was measured by liquid scintillation counting. Seven ^{32}P-labeled fractions were obtained. The potential phosphorylation sites in these seven fractions were deduced by covalent amino acid microsequencing as described above. T483 and T485 equivalents of rabbit HRI were again identified as phosphorylation sites of HRI (data not shown).

Thus, Thr483 and Thr485 in HRI were identified to be autophosphorylated by three independent methods. Thr483 and Thr485 are located in the activation loop of HRI between kinase domains VII and VIII and are conserved in HRI from mammals, chicken, xenopus, and fish (Table 1). However, only the T485 equivalent is conserved among all eIF2α kinases (Table 1).

Autophosphorylation of T485, but Not T483, Is Essential for the Attainment of the eIF2α Kinase Activity of HRI. Phosphorylation of the Thr residue(s) in the activation loop has been shown to be of great importance in many protein kinases such as PKA, CDK2, and MAPK (*35*) as well as PKR and GCN2 eIF2α kinases (*23*). We, therefore, have investigated the functions of the autophosphorylation of T483 and T485 by site-directed mutagenesis of these two residues individually to nonphosphorylatable Ala or negatively charged Asp that may mimic phosphorylation. The effects of these mutations in HRI were examined first by expressing the mutant proteins in *E. coli*.

We have shown recently that HRI species with different extents of autophosphorylation can be resolved by SDS−PAGE and analyzed by anti-HRI Western signals (*24*, *25*). As reported earlier (*24*, *25*), extensively phosphorylated Wt HRI migrated slower than the inactive K196R HRI (Figure 3A). The K196R HRI has a substitution of Lys196 for Arg in the kinase domain II and has been shown to be extremely poorly autophosphorylated (*24*, *25*). T483A and T483D were extensively phosphorylated and had an electrophoretic mobility similar to that of Wt HRI (Figure 3A). In contrast, T485A exhibited two phosphorylated species, and both species had a faster electrophoretic mobility than Wt HRI (Figure 3A). However, T485A still had a slower electrophoretic mobility than K196R (Figure 3A). Thus, T485A is autophosphorylated to a lesser extent than Wt HRI but is autophosphorylated to a greater extent than K196R. This result indicates that phosphorylation of T485 is not essential for the earlier steps of autophosphorylation and may occur

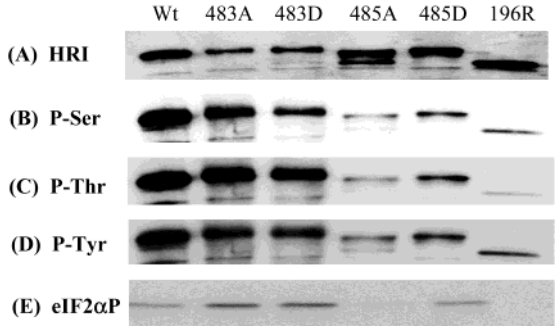

FIGURE 3: Autophosphorylation of T485 is required for the autokinase and eIF2α kinase activities of HRI. Wt, T483A, T483D, T485A, T485D, and K196R HRI mutants were expressed in *E. coli*. The extent of HRI autophosphorylation was examined by 7.5% SDS−PAGE and Western blot analysis using anti-HRI antibody (A) and antibodies against P-Ser (B), P-Thr (C), and P-Tyr (D), respectively. The eIF2α kinase activities of Wt and mutant HRI were determined by in vitro protein kinase assays using an equal amount of HRI protein (E).

at a later stage. T485D migrated slightly faster than Wt HRI but slightly slower than the upper band of T485A. Therefore, T485D is less autophosphorylated than Wt HRI but more autophosphorylated than T485A.

The extent of autophosphorylation of HRI was further validated with antibodies specific to phosphoserine (P-Ser), phosphothreonine (P-Thr), and phosphotyrosine (P-Tyr) (Figure 3B−D). T483A and T483D underwent autophosphorylation to an extent similar to that of Wt HRI, whereas T485A had much less autophosphorylation at Ser, Thr, and Tyr residues. Substitution of T485 with charged Asp resulted in a better autokinase activity than T485A, although the activity was still significantly less than Wt HRI. These results indicate that phosphorylation of T483 is not essential for HRI autokinase activity while autophosphorylation of HRI at T485 is necessary for a higher autokinase activity and the upshift to hyperphosphorylated HRI.

The eIF2α kinase activities of these mutant HRI were measured by in vitro eIF2α kinase assays. Our results showed that T483A, T483D, and T485D were active eIF2α kinases like Wt HRI (Figure 3E). However, the T485A, like K196R, had no eIF2α kinase activity. These results demonstrate that autophosphorylation of HRI at T485, but not T483, is required for attaining the eIF2α kinase activity.

To further establish the physiological functions of autophosphorylation of T483 and T485 of HRI, these mutant HRI were also expressed in human embryonic kidney 293T cells. T483A, T483D, and T485D were expressed at levels similar to that of the Wt HRI. In contrast, the T485A was expressed at a level much higher than Wt HRI and was similar to that of the inactive K196R (Figure 4, top). Previously, we have shown that Wt HRI expressed in Sf9 cells acts as an inhibitor of protein synthesis and shuts off its own synthesis (*30*). Thus, less active or inactive HRI is expressed at a higher level than the active Wt HRI. The high-level expression of the T485A suggests that it is less active than Wt HRI. This conclusion is further validated by in vitro eIF2α kinase assays of the Wt and mutant HRI.

There was endogenous eIF2α kinase in 293T cells, most likely PKR, which was activated by arsenite. The level of phosphorylated eIF2α was maximally elevated in the mock transfection without the overexpression of HRI. No further

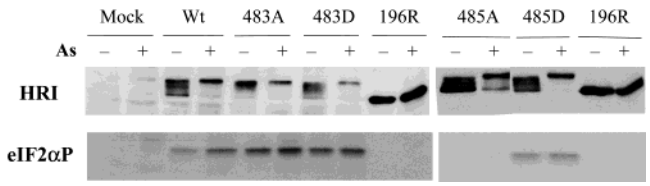

FIGURE 4: Autophosphorylation at T485 is essential for the arsenite-enhanced eIF2α kinase of HRI. Wt, K196R, T483, and T485 mutants were expressed in 293T cells for 48 h. Cells were then treated with or without arsenite. The activation of HRI was examined by 7.5% SDS−PAGE and anti-HRI Western blot analysis. The eIF2α kinase activities of Wt and mutant HRI in the S10 extracts were determined by in vitro eIF2α kinase assays using an equal amount of HRI proteins. The incorporation of ^{32}P into eIF2α was detected by autoradiography.

increase in eIF2αP was observed upon expression of HRI (data not shown). Therefore, the eIF2α kinase activities of the Wt and mutant HRI were determined by in vitro eIF2α kinase assays. As shown in Figure 4, T483A, T483D, and T485D were active eIF2α kinases while T485A was inactive and did not phosphorylate eIF2α (Figure 4, bottom). These results indicate that autophosphorylation at T485, but not T483, is also required for the activation of HRI in mammalian cells to obtain its eIF2α kinase activity. In addition, T485A was less autophosphorylated than Wt HRI, and most of T485A expressed was present as a faster migrating species. In contrast, T485D was present as a slower migrating species like Wt HRI. Thus, these results also demonstrated that autophosphorylation of T485 is required for the formation of the slower migrating species.

Autophosphorylation at T485 Is Necessary for Arsenite-Induced Activation of eIF2α Kinase Activity of HRI. We have shown recently that HRI can be activated by autophosphorylation during stresses other than heme deficiency. It is the only eIF2α kinase activated by arsenite treatment in erythroid cells (*25*). To determine whether autophosphorylation at T483 and T485 was involved in stress activation of HRI, 293T cells expressing these mutant HRI were treated with arsenite. As shown in Figure 4 (top), Wt HRI was upshifted completely upon arsenite treatment, indicating further autophosphorylation of HRI. The same observations were made for T483A and T483D. But this is not the case for the inactive K196R HRI which was not upshifted at all by arsenite treatment as shown previously (*25*). These results demonstrate that HRI is hyperphosphorylated upon arsenite activation by autophosphorylation in 293T cells as shown previously in Chinese hamster cells (*25*). In addition, the eIF2α kinase activities of the Wt, T483A, and T483D increased upon treatment with arsenite. These results indicate that autophosphorylation at T483 is not required for arsenite-induced activation of HRI since T483A is activated by arsenite in a manner similar to Wt HRI.

Interestingly, the majority of T485A was also upshifted upon arsenite treatment. As expected, T485D was upshifted and hyperphosphorylated like Wt HRI (Figure 4, top). These results show that autophosphorylation at residues other than T485 occurs upon arsenite activation of HRI and that T485 autophosphorylation is not required for further autophosphorylation upon arsenite activation. However, T485A remained inactive without eIF2α kinase activity upon arsenite treatment (Figure 4, bottom). Thus, autophosphorylation at T485 is also essential for attaining eIF2α kinase activity upon

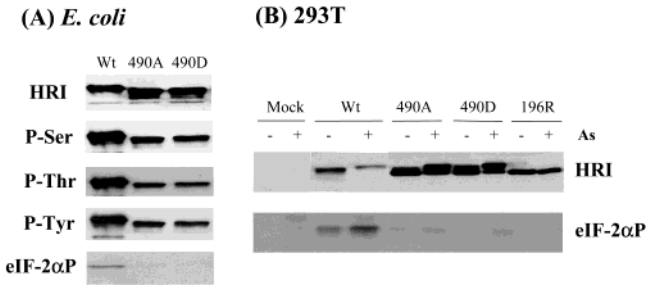

FIGURE 5: T490 is required for the last stage autophosphorylation of HRI and the activation of eIF2α kinase activity. T490A and T490D HRI were expressed in *E. coli* (A) or in 293T cells and then treated with or without arsenite (B). The extent of HRI autophosphorylation was analyzed by Western blot analysis using anti-HRI antibody and anti P-Ser, P-Thr, and P-Tyr antibodies as indicated. eIF2α kinase activities of Wt and mutant HRI were determined as described in the legend of Figure 3.

arsenite treatment. It is interesting to note that the eIF2α kinase activity of T485D was not increased by arsenite even though additional autophosphorylation occurs as Wt HRI. This result indicates that T485D is constitutively active and further supports the above notion that T485 phosphorylation is essential for obtaining eIF2α kinase activity.

T490 Is Critical for Autophosphorylation and Activation of HRI. In addition to T483 and T485, there is another conserved Thr, T490, in the activation loop of HRI (Table 1). The equivalents of T490 in PKR (Thr451) and in GCN2 (Thr887) have been shown to be important for PKR and GCN2 activities (*23*). We have investigated the function of the T490 in mouse HRI by site-directed mutagenesis to either Ala or Asp. Like T485A, both T490A and T490D had a faster electrophoretic mobility than the Wt HRI when expressed in *E. coli* (Figure 5A). Both T490A and T490D were also less autophosphorylated than the Wt HRI at Ser, Thr, and Tyr. In addition, both of these mutant HRI were inactive eIF2α kinases. These results demonstrate that T490 is required for a high autokinase activity and the eIF2α kinase activity of HRI. Therefore, like T485A, T490A and T490D are less autophosphorylated and cannot undergo the last stage of autophosphorylation which is necessary for attaining eIF2α kinase activity.

When expressed in mammalian 293T cells, T490A and T490D also had little to no eIF2α kinase activity even upon arsenite treatment (Figure 5B). Furthermore, both T490A and T490D underwent less autophosphorylation and migrated slower than Wt HRI. Only a fraction of T490 mutant HRI was upshifted and further phosphorylated upon arsenite treatment. These results showed that T490 was also required for increased eIF2α kinase activity and autokinase activity of HRI in response to arsenite. Since T490 is not identified as an autophosphorylated site, it seems that the T490 residue itself may be critical for catalytic kinase activity and may not be regulated by autophosphorylation. This conclusion is consistent with the result that Asp substitution at T490 is inactive (Figure 5), in contrast to T485D which is constitutively active (Figures 3 and 4).

T485 Phosphorylation Is Essential for the Hyperphosphorylation and Activation of HRI. To determine whether T485 was autophosphorylated in mutant HRI, an antibody raised against the HRI peptide phosphorylated at T485 (KGTRTHT^{485}[P]SRVGTC) was used to analyze which species of HRI was phosphorylated at T485. As shown in

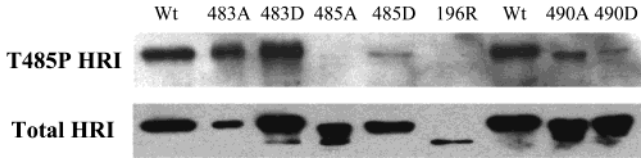

FIGURE 6: T485 is autophosphorylated at the last stage of HRI activation. Wt and mutant HRI were expressed in *E. coli*. The cell lysates were separated by 7.5% SDS−PAGE and analyzed for T485 phosphorylation and total HRI protein using antibody specific for the phosphorylayted T485 (T485P) HRI (top) and anti-HRI antibody (bottom), respectively.

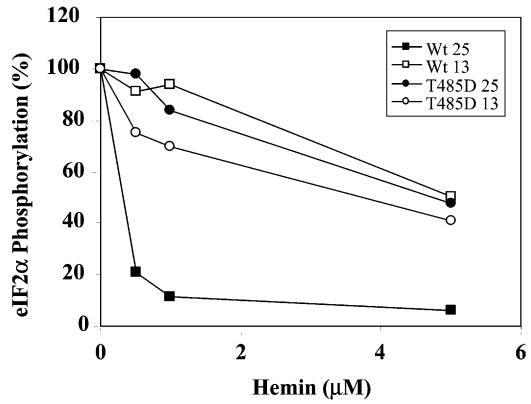

FIGURE 7: Loss of heme regulation of activated hyperphosphorylated HRI. Wt and T485D HRI were expressed at 13 or 25 °C overnight in *E. coli*. Inhibitions of eIF2α kinase activities of Wt and mutant HRI by heme were determined by preincubation of equal amounts of HRI protein with various concentrations of hemin (0−5 μM) prior to eIF2α kinase assays. The extents of the inhibition of eIF2α phosphorylation were visualized by autoradiography and quantitaed by scintillation counting of the gel slices corresponding to eIF2α. The amount of ^{32}P radioactivity of eIF2α at zero concentration of hemin was defined as 100%.

Figure 6 (top), anti-T485P HRI antibody was specific for HRI phosphorylated at T485. It recognized Wt, T483A, and T483D HRI. However, this antibody did not recognize T485A HRI, which could not undergo autophosphorylation at T485 because of the substitution of Ala for Thr, even though there was T485A protein present as detected by anti-HRI antibody which recognized all forms of HRI (Figure 6, bottom). Interestingly, anti-T485P antibody also recognized T485D HRI, albeit to a much lesser extent. Most importantly, T485P antibody did not interact with the faster migrating and less autophosphorylated HRI species seen in K196R, T490A, and T490D. Furthermore, T490A and T490D were very poorly autophosphorylated at T485 as compared to Wt, T483A, and T483D HRI. This poor autophosphorylation at T485 of T490A and T490D HRI correlates with their poor eIF2α kinase activities, providing further support for the above conclusion (Figure 4) that autophosphorylation at T485 is essential in order to attain the eIF2α kinase activity of HRI. Together, these results demonstrate that HRI is indeed autophosphorylated at T485 and that autophosphorylation at this site is essential for hyperphosphorylation and activation of HRI.

Loss of Heme Regulation of Activated HRI. We have observed that HRI expressed in *E. coli* at 13 °C was hyperphosphorylated and completely upshifted as compared to the HRI expressed at 25 °C. Interestingly, the eIF2α kinase activity of the HRI expressed at 13 °C became insensitive to heme regulation, in contrast to HRI expressed at 25 °C

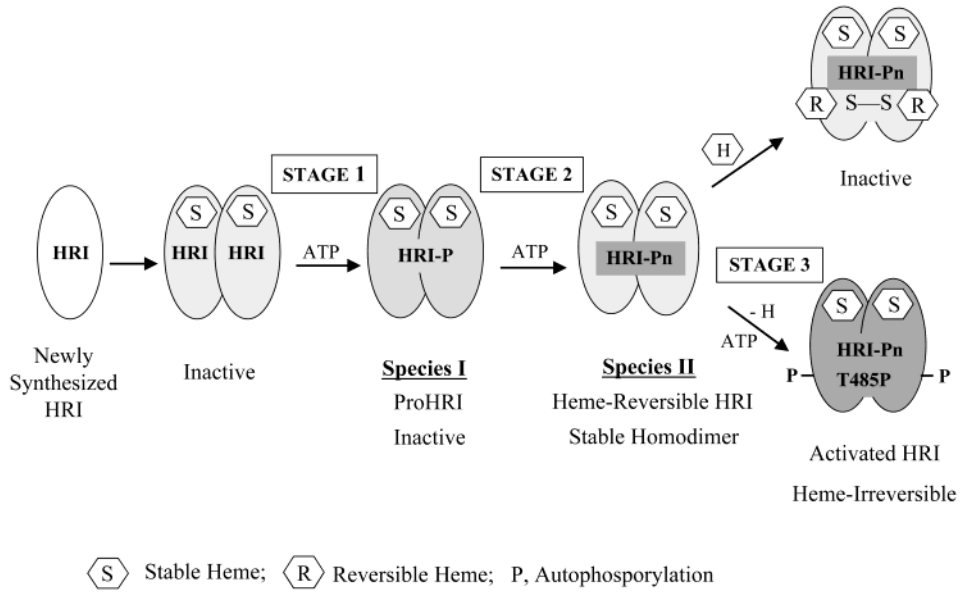

FIGURE 8: A model of the activation of HRI by multiple autophosphorylation in three stages.

(Figure 7). The apparent K_i of hemin increased 20-fold to 5 μM for 13 °C Wt HRI as compared to the apparent K_i of 0.2 μM for 25 °C Wt HRI. Thus, the activated hyperphosphorylated HRI is not regulated by heme.

The heme regulation of T483A, T483D, and T485D HRI has also been examined. T485A was inactive, and the heme regulation of eIF2α kinase activity could not be examined. The heme regulations of T483A and T483D were similar to that of the Wt HRI (data not shown). T485D expressed at either 13 or 25 °C, however, was relatively insensitive to heme (Figure 7). These results demonstrate that T485D is constitutively active and is no longer downregulated by heme, like activated Wt HRI expressed at 13 °C.

DISCUSSION

Although HRI has been known to undergo multiple autophosphorylation in heme deficiency (*24*, *31*, *32*), little is known about the autophosphorylation sites and their roles in the activation of HRI. In this report, we show that residues T483 and T485, located in the activation loop of HRI, are autophosphorylated (Figures 1 and 2). In addition, we demonstrate that autophosphorylation at T485, but not T483, is required for the activation of the eIF2α kinase activity of HRI in response to both heme deficiency and oxidative stress induced by arsenite (Figures 3 and 4).

Protein kinases form the largest known protein family and have conserved amino acids in 11 kinase domains. These conserved residues are important for the structure and function of the kinases (*36*). It has been shown that the catalytic activities of many protein kinases such as PKA, CDK2, and MAPK require phosphorylation of amino acid residues between domains VII and VIII known as the "activation loop" (*37*). The conformational changes induced by phosphorylation in this region play an important role in the conversion of inactive protein kinases to active protein kinases. Phosphorylation of these residues results in the relief of steric hindrance and stimulates binding of ATP, the binding of the peptide substrate, or the phosphoryl transfer reaction itself (*37*). Autophosphorylation of the HRI T485 equivalents in other eIF2α kinases, the T446 in PKR and the T882 in GCN2, has also been reported to be important for their activities (*23*). Thus, HRI, and more generally the eIF2α kinase family, belongs to the family of kinases that is activated by autophosphorylation in the activation loop. Most importantly, our present study demonstrates that this autophosphorylation of T485 occurs at the late stage of multiple phosphorylation of HRI and is essential for the activation of the eIF2α kinase activity of HRI (Figures 3 and 6).

In addition to T485, equivalents of the T490 of HRI are also conserved among all eIF2α kinases (Table 1) and are important for kinase activities of PKR and GCN2 (*23*). Mutation of T490 of HRI to either Ala or Asp resulted in reduced autokinase activity (Figure 5). T490A and T490D, like T485A, do not undergo maximal autophosphorylation (Figure 4) and are locked as species II (see model in Figure 8); therefore, they lack eIF2α kinase activity. Since T490 has not been identified as an autophosphorylation site of HRI, it is most likely that T490 per se may be critical for the catalytic activity. This position of T490 is conserved as Thr or Ser in all serine/threonine protein kinases. In the case of PKA, this conserved T201 is not phosphorylated, and the T201A mutant protein is also inactive (*38*). The crystallographic model of PKA shows that the hydroxyl group of T201 is within the hydrogen-bonding distance from the NH_3 group of Lys168. Lys168 is in contact of the γ-phosphate of ATP and is essential for phosphoryl transferase activity. In addition, T201 also bridges Lys168 to Asp166, which orients the substrate hydroxyl group to accept the γ-phosphate. Thus, T201 in pKA and its equivalent T490 in HRI are integral parts of the active site of protein kinases and are essential for the phosphotransferase activity of autophosphorylation and heterophosphorylation of the substrate as well as for anchoring the substrates (*39*).

Although we have identified that T483 of HRI is autophosphorylated, substitution of this residue to Ala or Asp does not alter the autokinase or eIF2a kinase activity (Figure 3). There is also no detectable difference in heme regulation or activation by arsenite (Figure 4). However, Thr483 is completely conserved in all known sequences of HRI from

fish to human (Table 1), suggesting an important role of this residue in the structure and function of HRI. The role of T483 autophosphorylation remains to be investigated. Interestingly, both T483A and T483D have higher eIF2α kinase activities than Wt or T485D HRI (Figures 3 and 4). The exact mechanism of how T483 mutation increases eIF2α kinase activities is not clear. It may be due to increased eIF2 binding to the mutant HRI or increased phosphotransferase activity of the mutant proteins.

Upon arsenite treatment, Wt HRI is activated by further autophosphorylation, including that of the T485 residue, and subsequently its eIF2α kinase activity is increased. Although T485D also undergoes further autophosphorylation and is upshifted upon arsenite treatment, the eIF2α kinase activity of T485D is not increased (Figure 4). Furthermore, T485D is not regulated by heme (Figure 7) and is, therefore, constitutively active.

The activation of HRI in heme deficiency from inactive ProHRI to heme-reversible HRI and heme-irreversible HRI has been speculated and described in earlier studies in the 1970s (reviewed in ref *40*). Our recent and present studies have begun to assign molecular identities to these various forms of HRI and to elucidate the molecular mechanism leading to the activation of HRI in heme deficiency to balance the globin synthesis according to heme availability.

On the basis of our findings in this study and previous studies, we propose that newly synthesized HRI is rapidly dimerized and undergoes intermolecular multiple autophosphorylation in three stages (Figure 8). In the first stage, autophosphorylation of newly synthesized HRI stabilizes the ProHRI (species I) against aggregation. Although ProHRI is an active autokinase, it still lacks eIF2α kinase activity. Additional multiple autophosphorylation in the second stage is required for the formation of stable dimeric heme-reversible HRI (species II). While the formation of stable heme-reversible HRI is achieved through autophosphorylation, hsp 90 and its cohort are also necessary for the acquisition of the autokinase activity of HRI (*26*, *41*, *42*). In heme abundance, heme binds to the heme-binding site in the kinase insertion and represses the activation of HRI through intersubunit disulfide formation. In the absence of heme, heme-reversible HRI undergoes the third and final stage of multiple autophosphorylation at sites including the critical T485 residue and attains eIF2α kinase activity. This hyperphosphorylated HRI is no longer regulated by heme. Autophosphorylation of HRI at residue T485 is, therefore, a committing step in which the heme-reversible HRI is converted to the heme-irreversible HRI. We suggest that this activated HRI may be inactivated by proteolytic degradation (Figure 8). We found no evidence for the dephosphorylation of activated HRI. No slower migrating and, thus, less phosphorylated HRI was seen; rather, a decrease in the amount of HRI was observed upon arsenite treatment. This conclusion is consistent with the earlier observation by Hunt that autophosphorylated HRI is very stable and is not dephosphorylated when added to reticulocyte lysates (*40*).

We have shown previously that HRI undergoes multiple autophosphorylations at Ser, Thr, and Tyr residues in stages (*24*). As shown here in our model, autophosphorylation at each stage provides specific functions for the stability, solubility, heme regulation, and autokinase and eIF2α kinase activity of HRI. In addition to T483 and T485, other autophosphorylated residues in HRI, as seen in Figure 1, have also been identified. The roles of autophosphorylation of these residues in the regulation of HRI are currently under investigation.

ACKNOWLEDGMENT

We thank Dr. Ed Diala and Dr. John Westwick at the eastern region of C.B.S. Scientific Co., Inc., for providing us with a modified Hunter protocol for separation of phosphopeptides. We also thank Dr. Blain White from Wayne State University for generously providing us with the antibody to the phosphorylated T485 peptide of HRI. Finally, we thank Dr. Bettina Bauer from our laboratory for the alignment of HRI from different species.

REFERENCES

1. Chen, J.-J. (2000) in *Translational Control of Gene Expression* (Sonenberg, N., Hershey, J. W. B., and Mathews, M. B., Eds.) pp 529−546, Cold Spring Harbor Laboratory Press, Cold Spring Harbor, NY.
2. Chen, J.-J., and London, I. M. (1995) *Trends Biochem. Sci. 20*, 105−108.
3. Clemens, M. J. (1996) in *Translational Control of Gene Expression* (Hershey, J. W. B., Mathews, M. B., and Sonenberg, N., Eds.) pp 139−172, Cold Spring Harbor Laboratory Press, Cold Spring Harbor, NY.
4. Krishnamoorthy, T., Pavitt, G. D., Zhang, F., Dever, T. E., and Hinnebusch, A. G. (2001) *Mol. Cell. Biol. 21*, 5018−5030.
5. Hershey, J. W. B. (1991) *Annu. Rev. Biochem. 60*, 717−755.
6. Jackson, R. J. (1991) in *Translation in Eukaryotes* (Trachsel, H., Ed.) pp 193−229, CRC Press, Orlando, FL.
7. Han, A. P., Yu, C., Lu, L., Fujiwara, Y., Browne, C., Chin, G., Fleming, M., Leboulch, P., Orkin, S. H., and Chen, J. J. (2001) *EMBO J. 20*, 6909−6918.
8. Meurs, E., Chong, K., Galabru, J., Thomas, N. S. B., Kerr, I. M., Williams, B. R. G., and Hovanessian, A. G. (1990) *Cell 62*, 379−390.
9. Hinnebusch, A. G. (1994) *Trends Biochem. Sci. 19*, 409−414.
10. Santoyo, J., Alcalde, J., Mendez, R., Pulido, D., and de Haro, C. (1997) *J. Biol. Chem. 272*, 12544−12550.
11. Sood, R., Porter, A. C., Olsen, D., Cavener, D. R., and Wek, R. C. (2000) *Genetics 154*, 787−801.
12. Harding, H. P., Zhang, Y., and Ron, D. (1999) *Nature 397*, 271−274.
13. Shi, Y., Vattem, K. M., Sood, R., An, J., Liang, J., Stramm, L., and Wek, R. C. (1998) *Mol. Cell. Biol. 18*, 7499−7509.
14. Kaufman, R. J. (2000) in *Translational Control of Gene Expression* (Sonenberg, N., Hershey, J. W., and Matthews, M., Ed.) pp 503−528, Cold Spring Harbor Laboratory Press, Cold Spring Harbor, NY.
15. Tian, B., and Mathews, M. B. (2001) *J. Biol. Chem. 276*, 9936−9944.
16. Dong, J., Qiu, H., Garcia-Barrio, M., Anderson, J., and Hinnebusch, A. G. (2000) *Mol. Cell 6*, 269−279.
17. Qiu, H., Dong, J., Hu, C., Francklyn, C. S., and Hinnebusch, A. G. (2001) *EMBO J. 20*, 1425−1438.
18. Chefalo, P., Oh, J., Rafie-Kolpin, M., and Chen, J.-J. (1998) *Eur. J. Biochem. 258*, 820−830.
19. Rafie-Kolpin, M., Chefalo, P. J., Hussain, Z., Hahn, J., Uma, S., Matts, R. L., and Chen, J.-J. (2000) *J. Biol. Chem. 275*, 5171−5178.
20. Taylor, D. R., Lee, S. B., Romano, P. R., Marshak, D. R., Hinnebusch, A. G., Esteban, M., and Mathews, M. B. (1996) *Mol. Cell. Biol. 16*, 6295−6302.
21. Zhang, F., Romano, P. R., Nagamura-Inoue, T., Tian, B., Dever, T. E., Mathews, M. B., Ozato, K., and Hinnebusch, A. G. (2001) *J. Biol. Chem. 276*, 24946−24958.
22. Taylor, D. R., Tian, B., Romano, P. R., Hinnebusch, A. G., Lai, M. M., and Mathews, M. B. (2001) *J. Virol. 75*, 1265−1273.
23. Romano, P. R., Garcia-Barrio, M. T., Zhang, X., Wang, Q., Taylor, D. R., Zhang, F., Herring, C., Mathews, M. B., Qin, J., and Hinnebusch, A. G. (1998) *Mol. Cell. Biol. 18*, 2282−2297.

24. Bauer, B. N., Rafie-Kolpin, M., Lu, L., Han, A., and Chen, J.-J. (2001) *Biochemistry 40*, 11543−11551.
25. Lu, L., Han, A. P., and Chen, J. J. (2001) *Mol. Cell. Biol. 21*, 7971−7980.
26. Uma, S., Hartson, S. D., Chen, J.-J., and Matts, R. L. (1997) *J. Biol. Chem. 272*, 11648−11656.
27. Uma, S., Thulasiraman, V., and Matts, R. L. (1999) *Mol. Cell. Biol. 19*, 5861−5871.
28. van der Geer, P., and Hunter, T. (1994) *Electrophoresis 15*, 544−554.
29. Vallette, F., Mege, E., Keiss, A., and Adesnik, M. (1989) *Nucleic Acid Res. 17*, 723−733.
30. Chefalo, P. J., Yang, J. M., Ramaiah, K. V. A., Gehrke, L., and Chen, J.-J. (1994) *J. Biol. Chem. 269*, 25788−25794.
31. Gross, M., and Mendelewski, J. (1978b) *Biochim. Biophys. Acta 520*, 650−663.
32. Fagard, R., and London, I. M. (1981) *Proc. Natl. Acad. Sci. U.S.A. 78*, 866−870.
33. Andersson, L., and Porath, J. (1986) *Anal. Biochem. 154*, 250−254.
34. Muszynska, G., Andersson, L., and Porath, J. (1986) *Biochemistry 25*, 6850−6853.
35. Johnson, L. N., Noble, M. E., and Owen, D. J. (1996) *Cell 85*, 149−158.
36. Hanks, S. K., and Hunter, T. (1995) *FASEB J. 9*, 576−596.
37. Johnson, L. N., Noble, M. E. M., and Owen, D. J. (1996) *Cell 85*, 149−158.
38. Moore, M. J., Kanter, J. R., Jones, K. C., and Taylor, S. S. (2002) *J. Biol. Chem. 277*, 47878−47884.
39. Madhusudan, Trafny, E. A., Xuong, N. H., Adams, J. A., Ten Eyck, L. F., Taylor, S. S., and Sowadski, J. M. (1994) *Protein Sci.3*, 176−187.
40. Hunt, T. (1979) in *Miami Winter Symposium: From Gene to Protein* (Russel, T. R., Brew, K., Schultz, J., and Haber, H., Eds.) pp 321−345, Academic Press, New York.
41. Shao, J., Grammatikakis, N., Scroggins, B. T., Uma, S., Huang, W., Chen, J. J., Hartson, S. D., and Matts, R. L. (2001) *J. Biol. Chem. 276*, 206−214.
42. Shao, J., Hartson, S. D., and Matts, R. L. (2002) *Biochemistry 41*, 6770−6779.

BI034005V